

Information encoding in an oscillatory network

Sentao Wang^{1,*} and Changsong Zhou^{1,2}¹*Department of Physics, Hong Kong Baptist University, Kowloon Tong, Hong Kong*²*Centre for Nonlinear Studies and The Beijing-Hong Kong-Singapore Joint Centre for Nonlinear and Complex Systems (Hong Kong), Hong Kong Baptist University, Kowloon Tong, Hong Kong*

(Received 30 November 2008; revised manuscript received 19 February 2009; published 9 June 2009)

Information encoding in a globally coupled network is studied. When the network is in an oscillatory state, the network activities are dominated by the intrinsic oscillatory current and the stimulus is poorly encoded. However, when the amplitude of the input signal is large, the input can still be well read from the population rate and the temporal correlation between spike trains. The underlying reason is that there exists a competition between the intrinsic correlation caused by the oscillatory current and the external correlation caused by the input signal. With small input signal, the rate code performs better than the temporal correlation code. Our results provide insights into the effects of network dynamics on neuronal computations.

DOI: [10.1103/PhysRevE.79.061910](https://doi.org/10.1103/PhysRevE.79.061910)

PACS number(s): 87.19.lj, 87.19.1l, 87.19.1s

I. INTRODUCTION

The brain has many different states such as waking, sleep, attention, and so on. It is a central issue in neuroscience to explore the interplay between intrinsically generated activity and the input from the external world. When the brain is in different functional states, neural response to the same stimulus can be totally different [1]. Even subtle change in network dynamics can cause large change in the output of the network [2]. A well-known example of the network dynamics in determining neural responsiveness is the effect of attention which can enhance neuronal response and selectivity, as well as behavioral performance [3].

Synchronized rhythmic oscillation, whose frequency ranges from several to several hundred hertz, is one common type of network dynamics in nervous systems [4]. It is widely believed that these oscillations are caused by the dynamic interplay between excitatory and inhibitory populations of neurons with inhibition playing a particularly important role [5]. But it is still not clear how the external signal interacts with network dynamics when the network is in an oscillatory state. Both experimentally and theoretically, it is shown that these oscillations can provide an additional phase relative to the background oscillation cycle to encode information [6]. In several recent theoretical studies, it is found that ongoing oscillatory activity can improve spike precision and stimulus discrimination based on the population spike-count response [7]. However, in these theoretical studies, the oscillation is obtained via imposing a rhythmic external current on each neuron, not arise from the intrinsic network dynamics. It is still an interesting topic to explore whether information can be faithfully encoded in a self-sustained oscillatory network. In nervous system, information is represented by the firing rate or by the precise spike time [8]. But it is still unclear how the two codes behave when the network is in the oscillatory state.

Here we study information encoding in a recurrent network consisting of coupled integrate-and-fire (IF) neurons.

With strong coupling strength, the network is in the oscillatory state. When stimulus is injected to such an oscillatory network, there exists a competition between the intrinsic oscillatory current and the signal. When the signal is weak, the network behavior is dominated by the synaptic current and the stimulus is poorly encoded. But the time when those packets of synchronous activities appear is still related to the input signal. With a large signal amplitude, the population rate can follow the input signal instantaneously. The rate code and the temporal synchrony code behave in a different way. When the input signal is small, the signal is better encoded by the population rate.

II. MODEL

The network we study is composed of $N=100$ IF neurons [9]. The dynamics of the network is described by the following equation:

$$\tau_m \frac{dV_i}{dt} = V_{rest} - V_i + I_0 + I_{syn} + s(t) + \eta_i(t). \quad (1)$$

Here, τ_m is the membrane time constant, V_i is the membrane potential of the i th neuron, V_{rest} is the resting membrane potential, I_0 is the external constant input, and I_{syn} is the synaptic current. $\eta_i(t)$ is the independent Gaussian colored noise with the correlation time set as 2 ms whose standard deviation is used to represent noise intensity D . The stimulus $s(t)$ is a Gaussian noise low-pass filtered at 50 ms and half-wave rectified whose standard deviation is the signal amplitude A [10]. Unless specified otherwise, A is set as 5. When the membrane potential V_i reaches threshold value V_{th} , a spike is generated and the membrane potential is reset to the resting potential at which it remains clamped for a 5 ms refractory period. The synaptic current I_{syn} takes the form

$$I_{syn} = \sum_{exci} g \frac{t-t_j}{t_{ex}} e^{-(t-t_j)/t_{ex}} + \sum_{inhi} rg \frac{t-t_j}{t_{in}} e^{-(t-t_j)/t_{in}}. \quad (2)$$

Here $t_{ex}=1$ ms for excitatory connections and $t_{in}=2$ ms for inhibitory connections, g is the excitatory coupling strength, t_j is the time point where the j th neuron fires, and r is the

*wangstzz@yahoo.com.cn

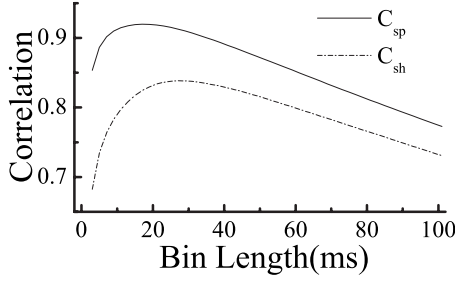


FIG. 1. The two correlation coefficients C_{sp} and C_{sh} versus the length of the time bin for $D=7$, $g=0$, and $A=5$.

ratio of the strength of inhibitory connection to that of excitatory connection set as 2.5 in order to make excitatory currents balanced with inhibitory currents. The network is coupled in an all-to-all manner. 80% of the connections between neurons are excitatory and 20% are inhibitory. Here $\tau_m=20$ ms, $V_{rest}=-60$ mV, $I_0=5$, and $V_{th}=-50$ mV. $I_{ex}(t) = \frac{1}{N} \sum_{exci} g_{ex} \frac{t-t_i}{t_{ex}} e^{-(t-t_i)/t_{ex}}$ is the averaged excitatory synaptic current. Numerical integration of these equations is performed by a second-order stochastic algorithm with a time step of 0.1 ms [11].

A moving time window of length L is used to account how many neurons of the network discharge spikes in this time bin. The time window is moving in the step of 1 ms. Such a temporal firing rate of the whole network is used to represent the output of the network. Here we call it spike time histogram (STH) [12]. The correlation coefficient C_{sp} between the input signal $s(t)$ and the STH $p(t)$ is used to quantify how well the input signal is encoded by the network [13]. C_{sp} is calculated as

$$C_{sp}(\tau) = \frac{\langle [p(t+\tau) - \bar{p}][s(t) - \bar{s}] \rangle_t}{\sqrt{\langle [p(t+\tau) - \bar{p}]^2 \rangle_t \langle [s(t) - \bar{s}]^2 \rangle_t}}. \quad (3)$$

Here the angular brackets denote an average over time. The value of τ , where the correlation coefficient is maximized, is the response delay of the network. For the maximal correlation in Fig. 1, the value of the response delay is equal to 1 ms. The peak value of the correlation coefficient is used to characterize the fidelity of rate code. To analyze what effects the intrinsic oscillation of the network has on information encoding, the correlation coefficient C_{si} between $s(t)$ and $I_{ex}(t)$ and the correlation coefficient C_{pi} between $p(t)$ and $I_{ex}(t)$ are also calculated in a similar way. An average over 50 different noise realizations is taken to obtain reported results.

The correlation between activities of different neurons can provide additional information about the input signal [14]. In order to see how the synchrony code behaves in the oscillatory network, a temporal synchrony is used to compute how much information is encoded by the precise spike time. A moving time window of length T is divided into small bins of $\Delta t=1$ ms. Two spike trains are given by $X(l)=1$ if one neuron spikes or 0 if it does not and $Y(l)=0$ or 1 for another neuron, with $l=1, 2, \dots, m$ (here $T/\Delta t=m$). The temporal synchrony is defined as

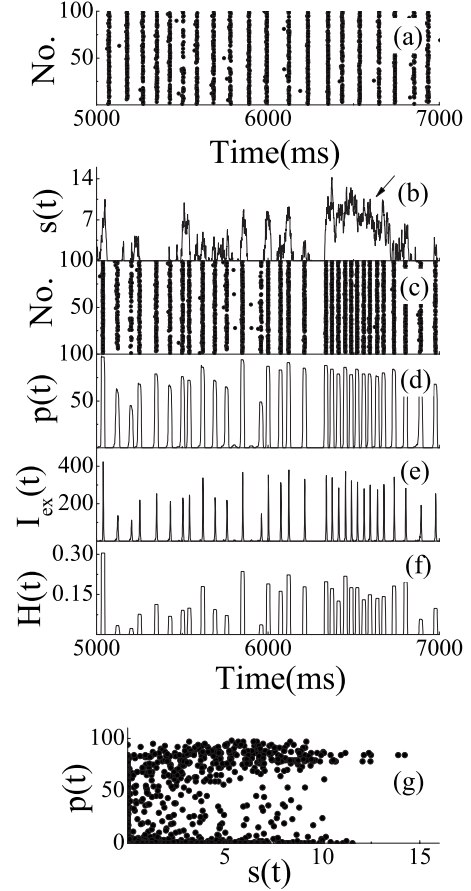


FIG. 2. $D=7$ and $g=20$. (a) Spike raster plots with $A=0$. [(b)–(f)] The input signal, spike raster plots, $p(t)$, $I_{ex}(t)$ and temporal synchrony $H(t)$ as a function of time with $A=5$. (g) Points sampled at 2 ms intervals taken from STH and the input signal.

$$H_{ij}(t) = \sum_{l=1}^m X(l)Y(l). \quad (4)$$

The population $H(t)$ is obtained by averaging over all pairs of the neurons in the network. The correlation coefficient C_{sh} between $s(t)$ and $H(t)$ is used to quantify how well the temporal synchrony between neural activities matches the input signal.

Obviously, the temporal synchrony $H(t)$ is not independent of the population rate $p(t)$. It has been found that the degree of synchrony between neuronal activities increases with firing rate [15]. In order to make a comparison of the two codes, the length T of the moving time window used to compute $H(t)$ is set equal to the length L of the moving time window used to compute $p(t)$. To choose a reasonable bin size, we plot the two correlation coefficients C_{sp} and C_{sh} versus the bin size with $g=0$ in Fig. 1. The value of the length 21 ms is chosen to make the two codes almost both optimized when there exist no couplings between neurons.

III. RESULTS

Figure 2(a) shows the spatiotemporal firing pattern with $g=20$ and $A=0$. Obviously, there exist some oscillations,

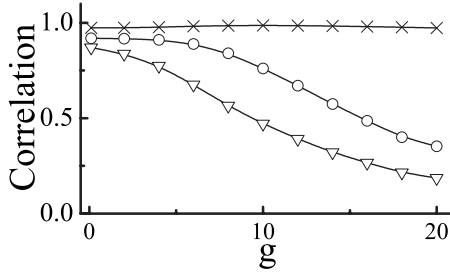


FIG. 3. $D=7$ and $A=5$. The correlation coefficient C_{sp} (\circ), C_{si} (∇), and C_{pi} (\times) versus the coupling strength g .

which can be confirmed by a peak located at about 10.5 Hz in the power spectrum of the network (data not shown here). With a weak signal injected to such an oscillatory network, the amplitude of the synaptic current is larger than that of the signal and the spike train of every neuron is dominated by the intrinsic synaptic current $I_{ex}(t)$ but not the weak signal. As a result, the output of the network $p(t)$ does not follow $s(t)$ linearly but $I_{ex}(t)$ [Figs. 2(b)–2(e)]. These synchronous firings are mainly caused by the intrinsic synaptic current [Fig. 2(f)]. That is, the weak signal cannot be read from the temporal synchrony $H(t)$. $p(t)$ is plotted versus $s(t)$ in Fig. 2(g). The dots are randomly distributed in the whole plane, meaning that the input signal cannot be encoded by the network when the network is in an oscillatory state. However, the time when these synchronous packets appear is still related to the input signal. When $s(t)$ has a large magnitude in a short time window [see the arrow in Fig. 2(b)], the number of synchronous packets of the network output in the corresponding time window is obviously larger than that in other time windows. It seems that there exists some competition between the external signal and the intrinsic oscillatory current. It is noted that in epoches of large signal, the neurons tend to fire with more correlation.

Figure 3 depicts the correlation coefficient C_{sp} , C_{si} , and C_{pi} versus the strength of excitatory connection g to clearly demonstrate the effect of oscillatory synaptic current on information processing. With the coupling strength increasing, C_{sp} and C_{si} decrease while C_{pi} almost keeps constant at 0.95. The underlying mechanism can be interpreted as follows. When the interplay between neurons is weak, the network activities are dominated by the independent noise and the signal. That makes the population firing rate follow the signal rapidly and faithfully. The synaptic current $I_{ex}(t)$ is only $p(t)$ filtered by the synaptic time course. Thus, $s(t)$, $p(t)$, and $I_{ex}(t)$ resemble each other and the signal can be well encoded by the network. As g increases, the amplitude of $I_{ex}(t)$ increases and the effect of $I_{ex}(t)$ on the membrane potential of each neuron becomes more evident. Therefore, the network activities are gradually dominated by $I_{ex}(t)$ and the intensity of the intrinsic oscillation also gradually increases. C_{sp} and C_{si} decrease and the precision of signal encoding decreases. With $g=20$, C_{sp} is less than 0.35 while C_{pi} is kept at 0.95, meaning that the outputs of the network contain quite less components of the signal $s(t)$ and are almost fully dominated by the intrinsic synaptic current $I_{ex}(t)$.

To clearly demonstrate the relationship between the intrinsic oscillation and information encoding, we use the STH

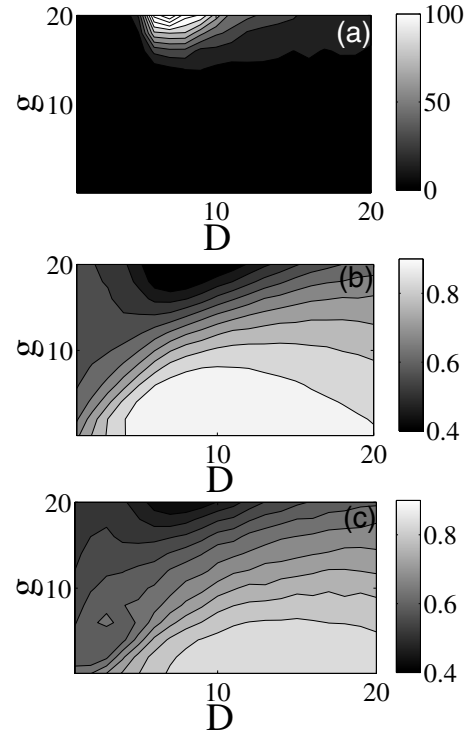


FIG. 4. (a) The STH variance σ^2 with $A=0$. (b) The correlation coefficient C_{sp} . (c) The correlation coefficient C_{sh} plotted as a function of the noise intensity D and the coupling strength g with $A=5$.

variance $\sigma^2 = \langle [p(t) - \bar{p}]^2 \rangle_t$ to quantify the degree of coherence of neural activities with $A=0$. When there is no collective oscillation of the whole network, $p(t)$ fluctuates around a constant value incoherently and σ^2 is small. σ^2 increases with the emergence of collective firing and oscillation, which arises from the interaction between the independent noise and the couplings [16]. The variance σ^2 , the correlation coefficient C_{sp} , and C_{sh} are plotted in Figs. 4(a)–4(c), respectively, as the coupling strength g and the noise intensity D are systematically varied. Compared with rate code, the temporal correlation behaves in a slightly different way, which will be discussed in the next paragraph. It can be clearly seen that, when the network is in an oscillatory state, the signal is poorly encoded by both the population rate $p(t)$ and the temporal synchrony $H(t)$. The precision of signal encoding decreases when the oscillatory intensity increases. The underlying reason is that, in the oscillatory state, the output of the network is dominated by the intrinsic synaptic oscillatory current as discussed above. For every value of g , there exists an optimal noise intensity level for rate code. Such a positive effect has been widely investigated and is generally termed “stochastic resonance” [17]. It is believed that it arises from the interplay between the nonlinearity of neurons and the noisy environment in nervous system [18]. For small noise currents, only when the signal is large, the neurons can fire. Therefore, all the neurons tend to discharge spikes at the same time. Since primarily independently firing neurons are required in rate code scheme, rate code is destroyed and the signal is poorly encoded by the population rate [Fig. 4(b)]. For intermediate noise intensity, the noise can help the neu-

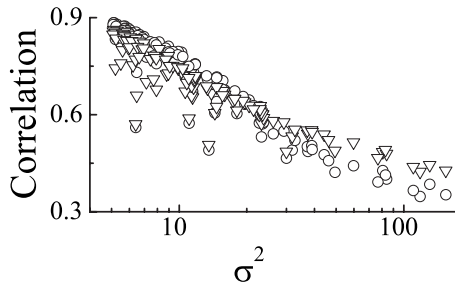


FIG. 5. The two correlation coefficients C_{sp} (○) and C_{sh} (▽) versus the STH variance σ^2 . The horizontal and vertical coordinate values of every data point correspond to the same values of the noise intensity D and the coupling strength g .

rons to go over threshold. The state of every neuron is much different when the signal arrives. As a result, the correlation coefficient C_{sp} is maximal since all the neurons almost fire independently. However, when the background current is too large, the background activity can overwhelm the weak signal. Therefore, the signal cannot be well read from $p(t)$. With g increasing, the optimal noise level increases, meaning that the neurons need more energy to go over threshold. For $g > 15$, due to the intense intrinsic oscillation, the value of the correlation coefficient C_{sp} is kept at a low level. With large value of the noise intensity, because the noise can destroy the intrinsic oscillation of the network, the signal can be better encoded. The relationship between the oscillatory intensity and information encoding is summarized in Fig. 5. Obviously, as the oscillation becomes more intense, the fidelity of both rate code and synchrony code decreases. With the same oscillation intensity, the fluctuation of the two correlation coefficients arises from different values of the noise intensity D or the coupling strength g .

In experiments, it has been shown that the synchrony between neural activities can be modulated by the input [19], meaning that the synchrony may play an important role in information encoding. In order to compare the rate code with the synchrony code, we plot the difference between C_{sp} and C_{sh} versus the noise intensity D and the coupling strength g in Fig. 6. If the difference is greater than 0, the rate code performs better than the synchrony code. Otherwise, the synchrony code performs better than the rate code. When both the noise intensity D and the coupling strength g are small, the rate code performs better. To clearly see what happens,

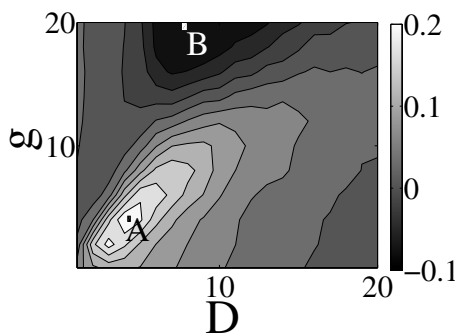


FIG. 6. $C_{sp} - C_{sh}$ as a function of the noise intensity D and the coupling strength g .

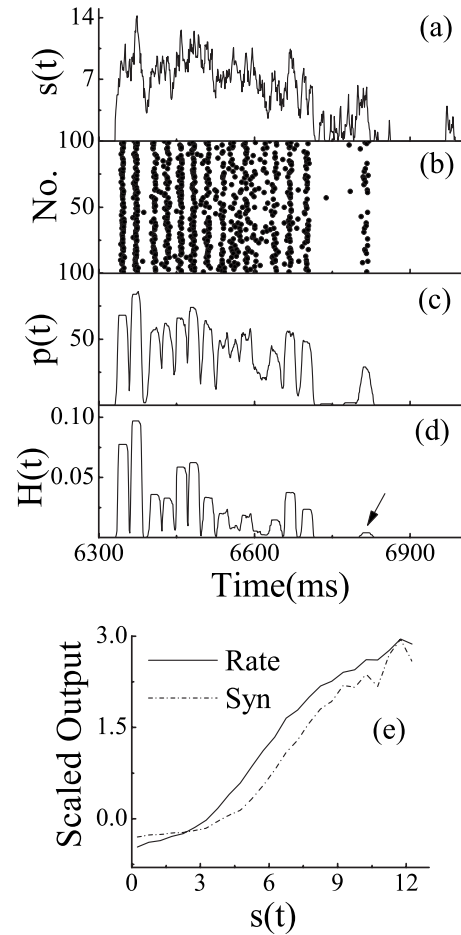


FIG. 7. Examples of point A in Fig. 6 with $D=4$ and $g=4$: (a) the signal. (b) Spike raster plots. (c) STH. (d) $H(t)$. (e) Scaled output versus the signal. First the code is rescaled according to Eq. (5). Then the two curves are obtained by averaging on the points with the same input signal.

one example ($D=4$ and $g=4$, point A in Fig. 6) is plotted in Fig. 7. With small value of D and g , the temporal synchrony does not follow the signal well when the input signal is low [see the arrow in Fig. 7(d)]. To exactly examine when the rate code performs better, we define a scaled output as

$$f(t) = \frac{f(t) - \bar{f}}{\sqrt{\langle [f(t) - \bar{f}]^2 \rangle_t}}. \quad (5)$$

Here $f(t)$ can be the rate code $p(t)$ or the synchrony code $H(t)$. Such a rescaling for the comparison of the rate code $p(t)$ and the synchrony code $H(t)$ is natural because it is used to compute the two correlation coefficients C_{sp} and C_{sh} [see Eq. (3)]. Then we plot the two scaled outputs versus the signal $s(t)$ as Fig. 1(g). After the points for the same $s(t)$ are averaged, we get the relationship between the two scaled codes and the signal $s(t)$ [Fig. 7(e)]. For $s(t) < 3$, with $s(t)$ increasing, the synchrony code almost keeps constant while the rate code increases more sharply. For $3 < s(t) < 5$, the rate code is much more sensitive to the input signal than the synchrony code. As a result, the signal is better encoded by the rate when the input signal is small. When the network is

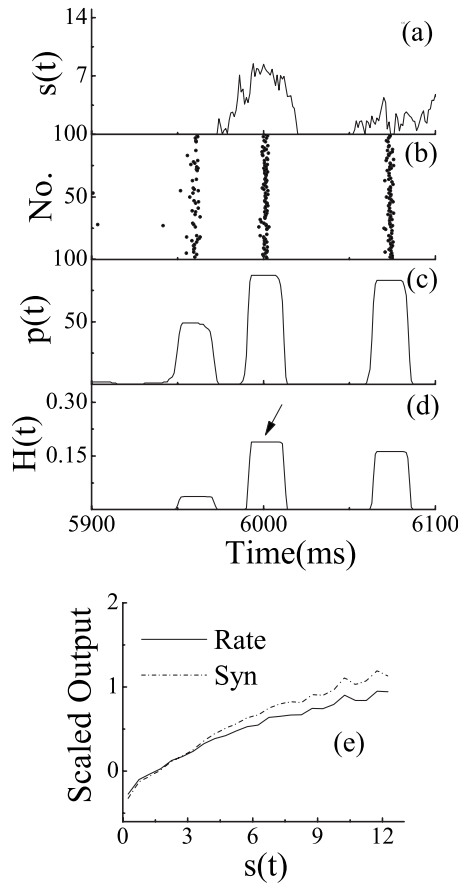


FIG. 8. Examples of point B in Fig. 6 with $D=7$ and $g=20$: (a) the signal. (b) Spike raster plots. (c) STH. (d) $H(t)$. (e) Scaled output versus the signal.

in the oscillatory state, the synchrony code performs a little better than the rate code. One example ($D=7$ and $g=20$, point B in Fig. 6) is plotted in Fig. 8. Without input signal, in some epoches, the network can produce spikes due to the external noise and the coupling. With input signal, both the rate code and the synchrony code increase, but the latter is more significant [see the arrow in Fig. 8(d)]. That is, with $s(t)$ increasing, the synchrony code increases more sharply than the rate code [Fig. 8(e)]. Therefore, the signal can be a slightly better read from the synchrony code.

To confirm our idea that there exists some competition between the intrinsic oscillatory current and the input signal, we change the amplitude of the signal which is injected to the oscillatory network. Spike raster plots and STH with different signal amplitude are shown in Figs. 9(b)–9(e). In the presence of the input signal, the number of synchronous packets increases as the signal amplitude increases, meaning that the time when synchronous packets appear is more related to the input signal [compare Figs. 9(b) and 9(d)]. Therefore, the signal is better encoded by the network [see Fig. 9(f)]. That is, the amplitude of $s(t)$ can determine whether the output of the oscillatory network follows the input. For every signal amplitude, when the coupling strength g is large, the signal is better encoded by the temporal synchrony because the synchrony code increases a little more sharply than the rate code as discussed above.

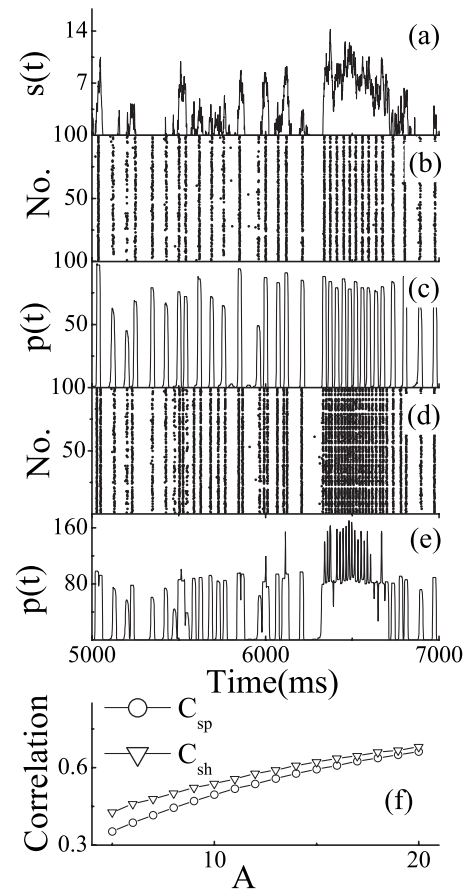


FIG. 9. The signal with different amplitudes injected to the oscillatory network. The value of the coupling strength is 20. (a) The signal versus time for $A=5$. (b) Spike raster plots and (c) STH for $A=5$. (d) Spike raster plots and (e) STH for $A=20$. (f) The two correlation coefficients C_{sp} and C_{sh} versus the signal amplitude.

IV. DISCUSSION AND CONCLUSION

In conclusion, we have investigated information encoding in a locally coupled network consisting of IF neurons. It is found that, when the network is in an intrinsic oscillatory state, the responsiveness to the input signal is weak. There exists a competition between the intrinsic current and the input signal. If the amplitude of the signal is large, it can still be well encoded by the output of the network. With small input signal, the signal can be better encoded by the rate code than the synchrony code.

Our result demonstrates that the oscillation has negative effects on information encoding if it arises from the intrinsic network dynamics. However, linear information code is not the only story in information processing of neuronal network. Synchronized firings that are still related to input signal may produce a new mapping and representation of the stimulus. Furthermore, these synchronous packets which are still related to the input signal can help information transmission between functional groups. In the working brain, many functional groups are often involved in the process of information encoding. The coherent rhythmic activities can be caused by the complicated interplay between functional groups. How the information is encoded in clustered oscilla-

tory network deserves a further study. The IF model used here is too simple to include any biological ion currents. It is noted that Parga and Abbott [20] extended the IF model by adding a nonlinear membrane current. The extended IF neurons can jump between up and down states, thereby producing bimodal membrane potential distributions, which has been widely discovered in experiments [21]. It is still open to explore how the rate code and the synchrony code behave when the network can jump between up and down states. It

has been shown that the two codes are affected oppositely by spike-frequency adaptation in a more biological model work [22].

ACKNOWLEDGMENT

This work was supported by Hong Kong Baptist University.

-
- [1] M. Steriade, *Neuronal Substrates of Sleep and Epilepsy* (Cambridge University Press, Cambridge, 2003).
- [2] A. Destexhe and D. Contreras, *Science* **314**, 85 (2006).
- [3] H. Spitzer, R. Desimone, and J. Moran, *Science* **240**, 338 (1988); G. M. Ghose and J. H. R. Maunsell, *Nature (London)* **419**, 616 (2002).
- [4] G. Buzsáki and A. Draguhn, *Science* **304**, 1926 (2004).
- [5] N. Brunel, *J. Physiol. (Paris)* **94**, 445 (2000); Y. Wang, D. T. W. Chik, and Z. D. Wang, *Phys. Rev. E* **61**, 740 (2000); D. Battaglia, N. Brunel, and D. Hansel, *Phys. Rev. Lett.* **99**, 238106 (2007); N. Brunel and V. Hakim, *Chaos* **18**, 015113 (2008).
- [6] M. R. Mehta, A. K. Lee, and M. A. Wilson, *Nature (London)* **417**, 741 (2002); J. J. Hopfield, *Proc. Natl. Acad. Sci. U.S.A.* **101**, 6255 (2004).
- [7] A. T. Schaefer, K. Angelo, H. Spors, and T. W. Margrie, *PLoS Biol.* **4**, e163 (2006); N. Masuda and B. Doiron, *PLOS Comput. Biol.* **3**, e236 (2007).
- [8] M. I. Rabinovich, P. Varona, A. I. Selverston, and H. D. I. Abarbanel, *Rev. Mod. Phys.* **78**, 1213 (2006).
- [9] A. Tonnelier and W. Gerstner, *Phys. Rev. E* **67**, 021908 (2003); A. Roxin, H. Riecke, and S. A. Solla, *Phys. Rev. Lett.* **92**, 198101 (2004); R. Moreno-Bote and N. Parga, *ibid.* **96**, 028101 (2006); P. Gong and C. van Leeuwen, *ibid.* **98**, 048104 (2007); E. Shea-Brown, K. Josic, J. de la Rocha, and B. Doiron, *ibid.* **100**, 108102 (2008).
- [10] M. C. W. V. Rossum, G. G. Turrigiano, and S. B. Nelson, *J. Neurosci.* **22**, 1956 (2002); T. P. Vogels and L. F. Abbott, *ibid.* **25**, 10786 (2005).
- [11] R. F. Fox, *Phys. Rev. A* **43**, 2649 (1991).
- [12] X. Pei, L. Wilkens, and F. Moss, *Phys. Rev. Lett.* **77**, 4679 (1996); S. Wang, J. Xu, F. Liu, and W. Wang, *Eur. Phys. J. B* **39**, 351 (2004); S. Wang, F. Liu, W. Wang, and Y. Yu, *Phys. Rev. E* **69**, 011909 (2004).
- [13] N. Masuda and K. Aihara, *Phys. Rev. Lett.* **88**, 248101 (2002).
- [14] R. C. deCharms and M. M. Merzenich, *Nature (London)* **381**, 610 (1996); J. W. Pillow *et al.*, *ibid.* **454**, 995 (2008).
- [15] J. de la Rocha, B. Doiron, E. Shea-Brown, K. Josic, and A. Reyes, *Nature (London)* **448**, 802 (2007).
- [16] C. Zhou, J. Kurths, and B. Hu, *Phys. Rev. Lett.* **87**, 098101 (2001).
- [17] A. Longtin, A. Bulsara, and F. Moss, *Phys. Rev. Lett.* **67**, 656 (1991); K. Wiesenfeld and F. Moss, *Nature (London)* **373**, 33 (1995); L. Gammaitoni, P. Hänggi, P. Jung, and F. Marchesoni, *Rev. Mod. Phys.* **70**, 223 (1998); A. Longtin and D. R. Chialvo, *Phys. Rev. Lett.* **81**, 4012 (1998); D. Nozaki, D. J. Mar, P. Grigg, and J. J. Collins, *ibid.* **82**, 2402 (1999); M. Rudolph and A. Destexhe, *ibid.* **86**, 3662 (2001).
- [18] A. Destexhe, M. Rudolph, and D. Pare, *Nat. Rev. Neurosci.* **4**, 739 (2003).
- [19] A. Kohn and M. A. Smith, *J. Neurosci.* **25**, 3661 (2005).
- [20] N. Parga and L. F. Abbott, *Front. Neurosci.* **1**, 57 (2007).
- [21] Y. Shu, A. Hasenstaub, and D. A. McCormick, *Nature (London)* **423**, 288 (2003); T. T. G. Hahn, B. Sakmann, and M. R. Mehta, *Proc. Natl. Acad. Sci. U.S.A.* **104**, 5169 (2007).
- [22] S. A. Prescott and T. J. Sejnowski, *J. Neurosci.* **28**, 13649 (2008).